Design and Implementation of an Open-Loop Solar Tracking System

By

Rafid Adnan Khan

And

M. Rezwanul Mahmood

Submitted to the

Department of Electrical and Electronic Engineering

Faculty of Sciences and Engineering

East West University

In partial fulfillment of the requirements for the degree of
Bachelor of Science in Electrical and Electronic Engineering
(B.Sc. in EEE)

Fall, 2016

Approved by

Thesis Advisor	Department Chairperson
Dr. Anisul Haque	Dr. Muhammed Mazharul Islam

Abstract:

Solar tracker, by directing a collector face towards the sun, can maximize energy extraction from solar system. There are different ways of solar tracking. In this thesis work we aim towards developing an open loop solar tracker that tracks the sun about single tilted axis with an optimum tracker rotation.

From time, date and location inputs taken into our device, we have calculated solar position using PSA (Platforma Solar de Almería) algorithm. From the calculated data we have optimized the single axis tracker rotation for maximum received solar radiation. We have implemented the optimum tracker rotation with a DC motor mechanically coupled with a linear multi turn wire-wound potentiometer. The potentiometer which is calibrated with respect to rotation angle sends a position feedback to the control unit. Depending on the given position feedback the control unit terminates the rotation at the required position (representing the respective optimum rotation angle) and goes through a definite interval. Thus the sun is tracked at certain intervals. In the design the robustness and reliability of the system has been emphasized. Finally we have experimentally analyzed the accuracy of tracking rotation and improved energy harvesting by tracking. The errors in angle range within ±5°. On a 30% overcast day, we have obtained 21% more energy by the designed tracking panel system with respect to a fixed panel system.

Acknowledgement

We would like to thank our supervisor, Professor Dr. Anisul Haque, Department of Electrical and Electronic Engineering, East West University, (EWU), Dhaka, Bangladesh for his suggestions and support to work on this topic.

We would also like to thank our Department Chairperson Dr.Muhammed Mazharul Islam and our academic advisors, Dr. Mohammad Mojammel Al Hakim and Mariam B. Salim for their encouragement and help.

We appreciate our parents and our friends for their support and concern in this thesis.

Authorization page

We hereby declare that we are the sole author of this thesis. We authorize East West University to lend this thesis to other institutions or individuals for the purpose of scholarly research.

_____

Rafid Adnan Khan

_____

M. Rezwanul Mahmood

We further authorize East West University to reproduce this thesis by photocopy or other means, in total or in part, at the request of other institutions or individuals for the purpose of scholarly research.

_____

Rafid Adnan Khan

_____

M. Rezwanul Mahmood

Table of Contents

List of Figures

List of Tables

Chapter 1:

Introduction:

Primarily the decline of fossil fuel resources and rise of global warming is drawing our attention to extract energy from renewable resources. Solar energy is one of the major sources of renewable energy. Using solar cells the incoming solar energy can be converted to electrical energy. Over the years, extensive researches have been conducted to improve the efficiency of photovoltaic systems. In this regard, solar tracking has drawn substantial research interest.

1.1 Background:

Solar flux that strikes a collector consists of direct-beam radiation, diffused radiation and reflected radiation. G. M. Masters has discussed the effects of these radiations on the collector surface [1]. Direct-beam radiation is solar radiation that travels in a straight line through the atmosphere to the receiver. Diffused radiation is solar radiation that has been scattered by molecules and particles in the atmosphere but still makes it down to receiver, and reflected radiation has been reflected from the ground or other surface in front of the collector to the collector. The contribution from the direct beam radiation increases proportionally to the cosine of incidence angle, the angle between collector face normal and incoming solar beam. So for minimum incidence angle the contribution from the direct beam radiation will be maximum. The incidence angles over the day can be minimized by introducing a control mechanism that aligns the collector orthogonally to the sun, which is called solar tracking. On the other hand, considering roughly equal distribution of diffused radiation throughout the sky, the steeper the solar panels are inclined the lesser is the diffused radiation on the solar panel for facing the lesser portion of the sky. So, a horizontal panel facing the whole sky will receive maximum diffused radiation.

As solar tracking involves inclining the collector face towards the moving sun, it will reduce the contribution from diffused radiation. Still, because direct radiation is much more intense than diffused radiation, the amount of contribution from diffused radiation reduced by inclining the solar panels is generally over compensated by the contribution from extra direct beam radiation gained by solar tracking. So, theoretically solar tracking has potential for improved energy harvesting for the maximizing the contribution from more intense direct beam radiation.

1.2 Literature review:

Substantial studies have been conducted to test the potential of solar tracking. Bingol *et al.* proposed and tested a micro-controller based two-axis solar tracking system and found out that rotary panel in this system received more light intensity than stationary panel [2]. Kivrak *et al.* designed a solar tracker, measured and simulated its performance with respect to a fixed panel system. They showed that more power was generated by the tracker system than the fixed panel system [3]. Huang *et al.* also showed similar outcome by carrying out a real life comparative test for several days using a fixed solar panel and a 1axis-3 position tracking solar panel. In a typical clear day their model could generate 34.6% more electricity than fixed solar panel [4]. From these discussions and experimental studies, solar tracking evidently has theoretical and practical potential for improved energy extraction from the sun.

There are various types of solar tracking system. In the context of this thesis, we can classify solar tracking system into two types based on feedback mechanism. One of the types is closed

loop solar feedback based tracking system that actively takes dynamic feedback from the sun to orient the collector orthogonally towards the sun. The other type is open loop tracking system that calculates the sun position based on location, time, then at intervals determines and implements the appropriate tracker rotation depending on the pre-calculated solar position and known tracker position. Depending on degree of freedom in solar tracking it can be further classified into single axis solar tracking system with only one degree of freedom and dual axis solar tracking system with two degrees of freedom. This thesis work deals with the open loop single axis solar tracking system.

Solar position is determined by mainly two angles, one is solar altitude or zenith angle and the other is solar azimuth angle. Solar map equations help determine these two angles if time, date and geographical location of a place are provided. Using this concept, Karim *et al.* designed an arduino based dual axis solar tracking system for a fixed location. The arduino calculated the solar angles, converted these results into motor movement and rotated the panel in both axes by servo motors. The azimuth and altitude angle readings were taken from calculations and hardware model respectively and compared with the data obtained from NREL (National Renewable Energy Laboratory) website for a particular date. The angle errors were within tolerable range [5].

Rashid *et al* built another open loop dual axis tracking system comprising of computer, DAQ (Data Acquisition) card, relays, lead acid battery and motors. The system converted time, date and geographical location into solar angles and then rotated the panel accordingly. It also computed solar irradiance received perpendicularly by the panel surface to find out higher energy gained [6]. Besides, there have been many more studies and projects on open loop predetermined solar tracking.

This thesis work aims towards extending the domain of open loop solar tracking system for tilted single axis applications using optimum tracker rotation angle, which is calculated on solar position and tracker axis position [7]. The optimization to single axis rotation leads to lower cost and enhanced economic scalability. Besides, we will use DC motor mechanically coupled with a linear multi turn wire-wound potentiometer for motor position feedback. The use of servo motor in the previous studies limit the economic scalability of the systems as servo motor for large scale application can be expensive.

The arduino based solar tracking control system designed by Karim *et al.* [5] does not have location specific data input mechanism and user interface for device initialization. As the inputs are set as default in the program, it is difficult to incorporate the device for a changed location or positioning of the tracker. The research of Rashid *et al.* [6] involves device initialization through input of location parameters, time and date with the help of computer software as user interface. The whole system is based on data acquisition card and computer which imposes the limitation upon the economic scalability and application of the designed system.

1.3 Objectives

The objective of our work is to maximize the extractable solar energy from a PV (photovoltaic) panel by designing an open loop single axis solar tracker, analyze its performance and experimentally demonstrate improved energy harvesting with the implemented design.

In our system we will introduce data input mechanism where the inputs are provided to the system by push button switches and displayed with the help of an LCD (Liquid Crystal Display).

This user interface mechanism is economical compared to the total system installation cost. It also allows the user to adjust latitude, longitude, tracker tilt angle, time and date for setting up the system as required. Thus the system is usable at any location with any optimized tilt angle.

1.4 Thesis Organization

This thesis report contains seven chapters. Chapter 1 introduces solar tracking and discusses its purpose and previous studies conducted on this topic. It also includes the objectives of our work on open loop solar tracking system. Chapter 2 discusses classification of solar tracker depending on axes and feedback mechanisms and also relative advantages and disadvantages of different types of solar trackers. Chapter 3 discusses solar positioning angles, illustrates the comparison among different solar position algorithms that determine solar positioning angles and states algorithm selected for this thesis work. Then it discusses tracker angles, adjustment of tracker tilt angle for maximizing energy and determination of optimum tracker rotation angle corresponding to maximum radiation. Chapter 4 describes system design, working algorithm of the system and components used for making the prototype. In Chapter 5 the analysis of the performance of the solar tracker rotation is provided. Chapter 6 shows the improved energy harvested by the solar tracker along with experimental process and results. Chapter 7 summarizes our work on open loop tracking system and mentions its further developments. References and appendix are included at the end of the thesis report.

Chapter 2:

Context Based Tracker Classification:

2.1 Solar tracker Types Depending on Axes:

2.1.1 Single Axis Trackers:

Single axis tracker tracks the sun with one degree of freedom, about a single axis of rotation; the axis of rotation is generally north-south axis, as shown in figure 2.1.

To maximize solar irradiance on the collector, the axis can be inclined to an optimum tilt angle. The tilt angle depends on the location, panel position and time of the year. In northern hemisphere, the panel is tilted towards south and in southern hemisphere panel is tilted towards north to get better solar irradiance.
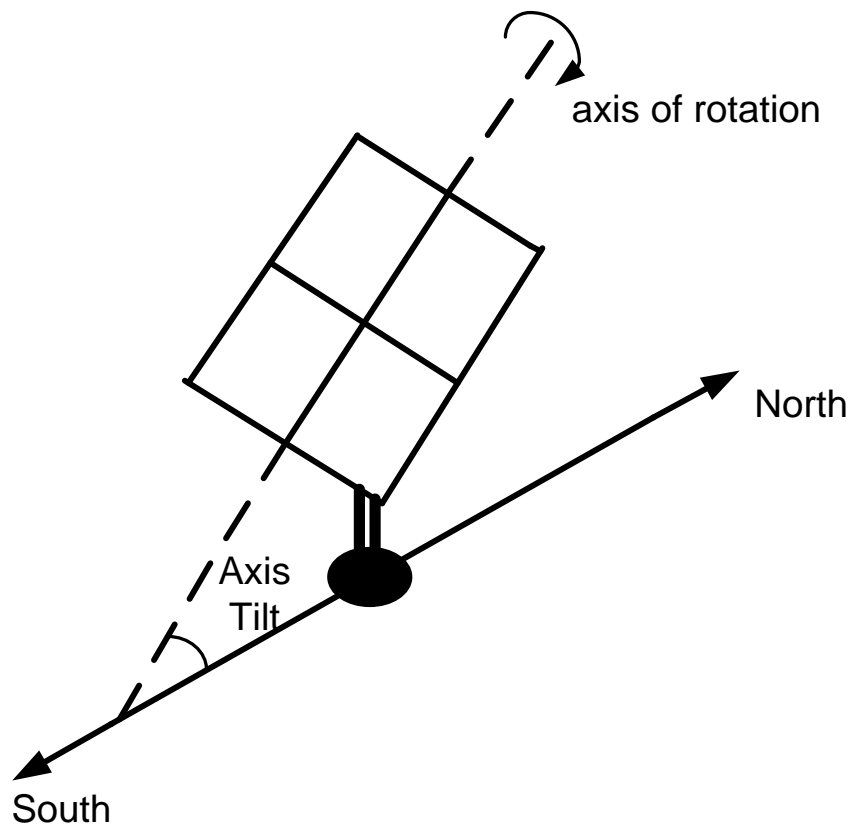
Figure 2.1: Schematic diagram of a tilted single axis tracker.

2.1.2 Dual Axis Tracker:

Dual axis tracker tracks the sun with 2 degrees of freedom, centering two respective rotation axes which are typically normal to each other. The axis that is connected to the foundation is referred as the primary axis and the axis that is connected to the primary axis is referred as the secondary axis. Figure 2.2 represents schematic view of a dual axis tracker.
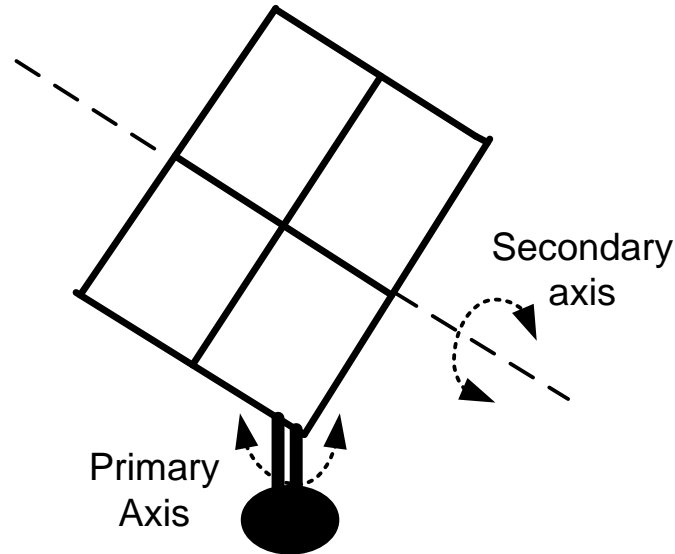
Figure 2.2: Schematic diagram of a dual axis tracker.

2.1.3 Comparison of single axis and dual axis tracker:

Single axis tracker, with one degree of freedom uses a relatively simple one dimensional mechanical configuration and control system. It has only one motor driver and motor. Energy loss associated with mechanical movement is minimum in single axis trackers. Besides with respect to dual axis tracker it costs relatively less for simple construction and fewer components. However, single axis tracker has relatively lower accuracy in solar tracking compared to that of dual axes tracker. Also single axis tracker cannot account for seasonal changes. So the improvement in energy extraction through tracking is slightly lower compared to that of dual axes tracker. The accuracy of single axis solar tracking can be slightly improved by tilt angle optimization and manual adjustment of the optimum tilt angle on monthly or seasonal basis, depending on convenience.

On the other hand, dual axes tracker is relatively accurate in solar tracking with its two degrees of freedom, it can account for seasonal changes. So the improvement in energy extraction through tracking is slightly more than the single axis tracker but at the compensation of increased cost and complexity of mechanical structure and control system. Dual axes tracker uses a two dimensional control system with two motor drivers and two motors. The improvement in energy harvesting by a dual axes tracker with respect to a single axis tracker in a particular region needs to be considered relative to its added cost and complexity before dual axes tracker installment in that region.

2.2 Solar tracker Types Depending on Feedback Mechanism:

2.2.1 Closed Loop Sensor Based Solar Tracking:

The solar tracker actively takes dynamic feedback from the sun using sensors to orient the collector orthogonally towards the sun. Figure 2.3 represents block diagram of an LDR (Light Dependant Resistor) sensor based closed loop solar tracking system which is designed by Wang and Lu [8]. The feedback controller consists of LDR sensors, differential amplifier and comparator. The LDR sensors generate voltages by absorbing sunlight. The unbalance in LDR

voltages generate an error voltage which is then compared by the comparator with respect to a specified threshold. If the comparator goes HIGH logic, the motor driver and relay will be turned on and rotate the panel. During this rotation, the feedback controller will calculate the error voltage. When the error voltage is less than the specified threshold, the comparator will go LOW logic and turn off the motor driver and delay and the rotation stops orienting the collector towards the sun orthogonally.
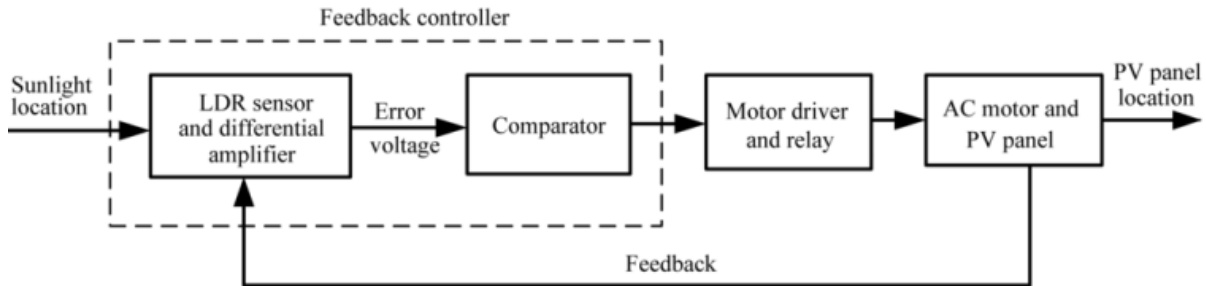
Figure 2.3: An LDR sensor based closed loop solar tracking block diagram.

2.2.2 Open Loop Solar Tracking:

The solar tracker system calculates the sun position based on location, time, date using solar position equation or look-up table of solar position. Then it determines and implements the appropriate tracker rotation depending on the pre-calculated solar position and known tracker position. Figure 2.4 summarizes this operation with the help of block diagram.

There is no sensor based solar position feedback in open loop solar tracking, the feedback, if employed can be for motor position control.
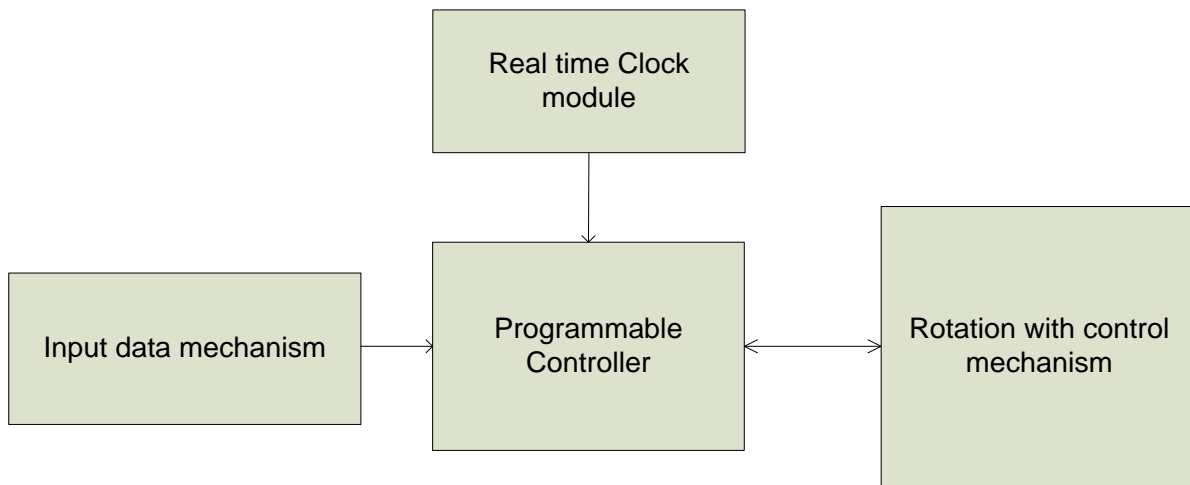
Figure 2.4: Block diagram an open loop solar tracking system.

2.2.3 Comparison of closed loop and open loop solar tracking systems:

Closed loop tracking system is sensitive to disturbances like reflection and shading. In case of such disturbances it may fail to track the sun. On the other hand, open loop tracking system is immune to disturbances like shading or reflection and so it will track the sun successfully. Closed loop tracking system uses a relatively complex circuit structure whereas open loop tracking system uses a much simpler circuit configuration.

Closed loop tracking system is based on dynamic feedback from the sun. Light dependent resistor or photo transistor, operational amplifier are used for its low cost implementation. It does not require complex mounting. As it tries to track the sun from any given position, small errors in mounting or small disruption in position of the tracker due to shock will not affect its performance. However open loop tracking system requires a computing hardware, calibrated linear position sensor, a data input mechanism with user interface which can increase the cost. It also tracks the sun position with respect to the tracker position. If errors of small magnitude occur in tracker mounting or tracker positioning, performance of the system may be affected. Thus such system requires more complex and rigid mounting of the tracker with respect to that of the tracker closed loop tracking system.

Chapter 3:

Predetermination of Single Axis Solar Tracker Position:

3.1 Solar Positioning Angles:

Solar positioning angles and tracker angles:

The position of the sun can be determined mainly from two angles, one is solar azimuth angle γ_s and the other is solar zenith angle θ_z or elevation angle ε.

Solar azimuth angle:

γ_s can be defined as the horizontal angle at which the sun rays are projected upon the surface, measured with respect to either north or south direction. In this thesis, the north direction is considered as reference and the angle values are positive in clockwise direction. γ_s is shown in figure 3.1.
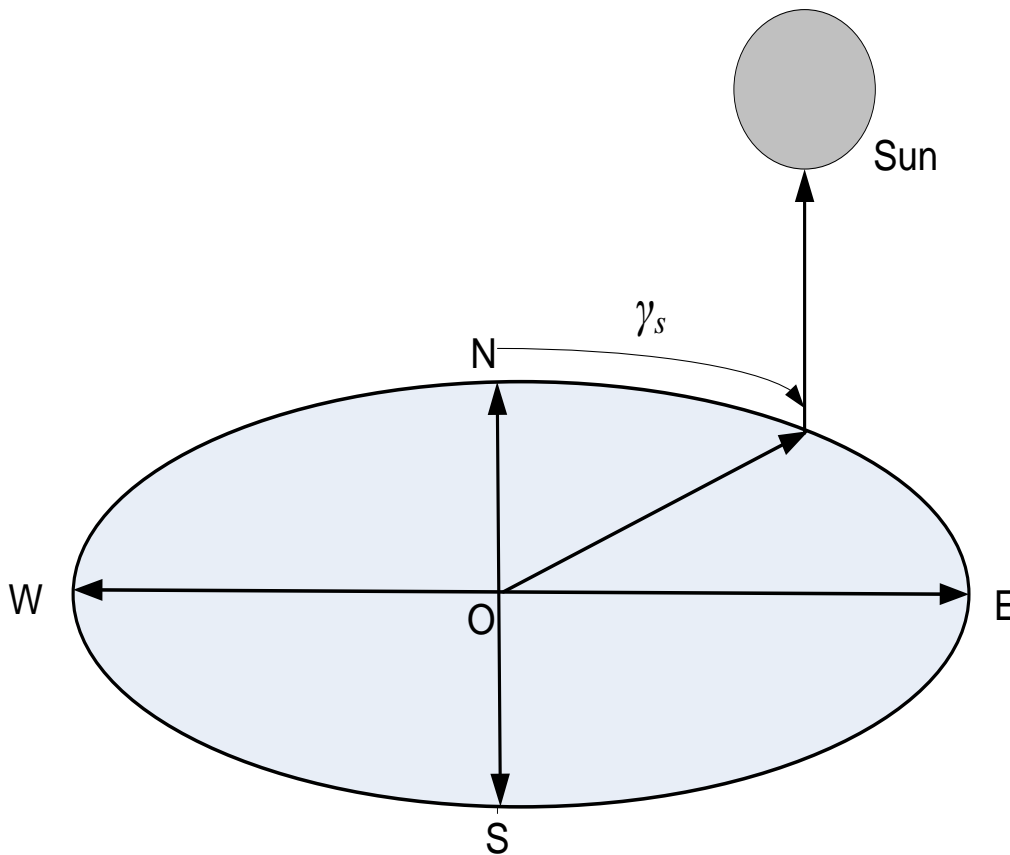
Figure 3.1: Schematic diagram of azimuth angle.

Solar zenith and elevation angle:

θ_z is the angle between solar rays and vertical of the observer point. ε is the angle between solar rays and horizontal surface at a particular point and determines the angular height of the sun from the surface. According to the figure 3.2, $\theta_z = 90 - \varepsilon$. That is θ_z is the complement of ε.
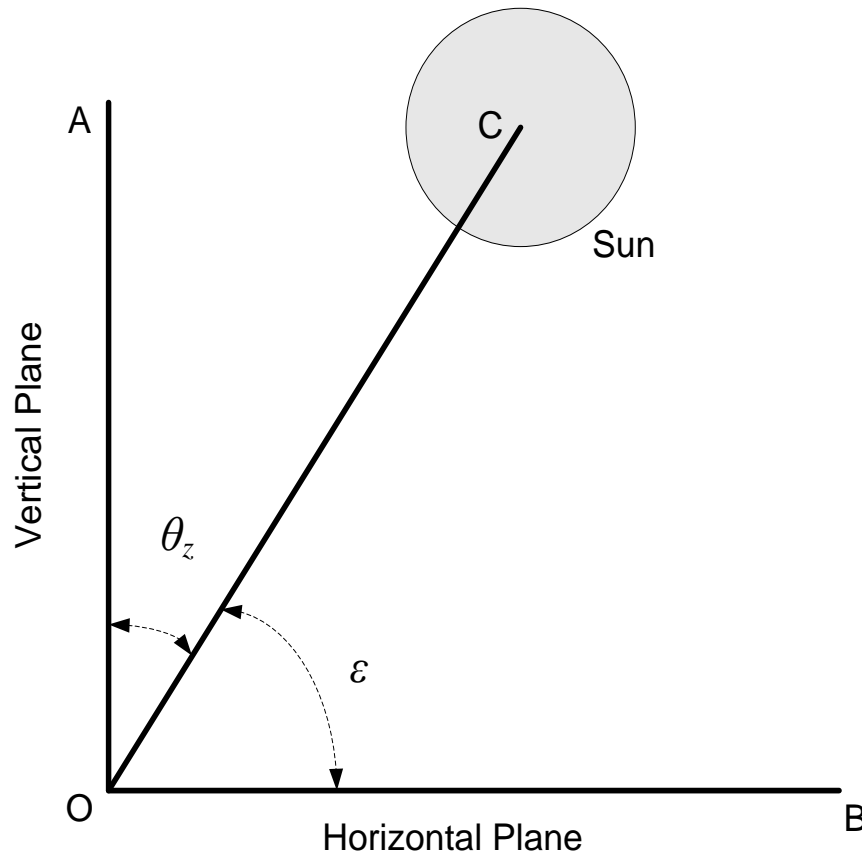
Figure 3.2: Schematic diagram of zenith or elevation angle.

3.2 Solar Position Algorithms:

3.2.1 A Comparative Overview:

Solar positioning algorithms can determine the solar zenith and azimuth for a given location and a given time. Numerous algorithms have been developed for positioning the sun with a tradeoff between accuracy and complexity. A rough comparison for complexity can be made by how many times the algorithms calls off trigonometric functions, direct or inverse. A few major recent solar position algorithms are compared and represented in table 3.1.

Table 3.1: Comparison among solar position algorithms.

Algorithms:	Uncertainty/Accuracy	Complexity:	Validity period of proposed accuracy:
SPA(Solar Position Algorithm)- NREL(National Renewable Energy Laboratory) Proposed by Meeus (1988) [9] reviewed by Reda and Andreas (2004) for suitable application [10]	± 0.0003° of uncertainty both in zenith angle and azimuth angle [10] with respect to the angles calculated by using AA (Astronomical Almanac) [11] parameters in exact trigonometric functions	Computationally more complex and slower. [12]	-2000 to 6000 year [10]
Michalsky (1988) [13]	Quadratic error (defined as the square root of the mean squared error) of 0.0031° in zenith angle and 0.0036° in azimuth angle [12] with respect to SPA-NREL algorithm	Multiple times Faster than SPA, 10% faster than Grena (2008) [12]	1950-2050 year [13]
PSA Algorithm (Blanco-Muriel *et al.*, 2001) [14]	Quadratic error of 0.00178° in zenith angle and 0.0029° in azimuth angle [12] with respect to SPA-NREL algorithm	Multiple times faster than SPA, 25% faster than Grena (2008) [12]	1999-2015 year [14]
Grena (2008) [12]	Quadratic error of 0.000556° in zenith angle and 0.001° in azimuth angle [12] with respect to SPA-NREL algorithm	Multiple times faster than SPA, but slower than Michalsky and PSA Algorithm [12]	2003-2023 year [12]

In 2012, Grena has published five optimized algorithms having five different levels of complexity being in trade off with accuracy, to meet the requirements in variable applications [15].

3.2.2: Selected Solar Position Algorithm:

In this thesis work, for positioning the sun, PSA (Plataforma Solar de Almería) algorithm (Blanco-Muriel *et al.*, 2001) is used [14]. The PSA algorithm takes longitude, latitude, GMT (Greenwich Mean Time) and date as input and gives solar zenith and azimuth angle for given

parameters as output. Here, to analyze the single axis tracking implementation performance, SPA-NREL algorithm obtained data is considered as bench-mark.

3.3 Tracker Angles:

Angle of incidence:

The angle formed at a point by the sun rays and the line normal to the collector surface is called incidence angle θ. Figure 3.3 represents θ.
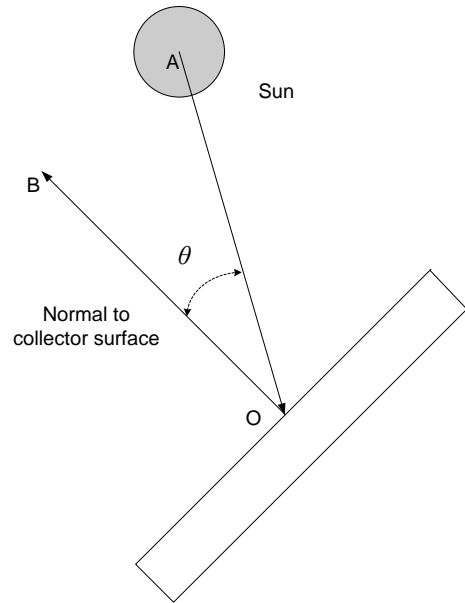
Figure 3.3: Schematic diagram of incidence angle.

Axis tilt:

Axis tilt β_a can be defined as inclination of the tracker axis from horizontal surface. It ranges from 0° to 90°. Figure 3.4 shows β_a.

Rotation angle:

It is the angular displacement of the collector rotating about its axis with respect to a reference position. In this thesis, when the normal to collector surface is parallel to vertical plane, the position is considered as the reference position, where rotation angle is zero degree. Rotation angle is positive for clockwise rotation and negative for counterclockwise rotation. In figure 3.4, R is rotation angle.

Axis azimuth:

It is the angle of the horizontal projection of tracker axis with respect to true north. In figure 3.4, γ_a is the axis azimuth.
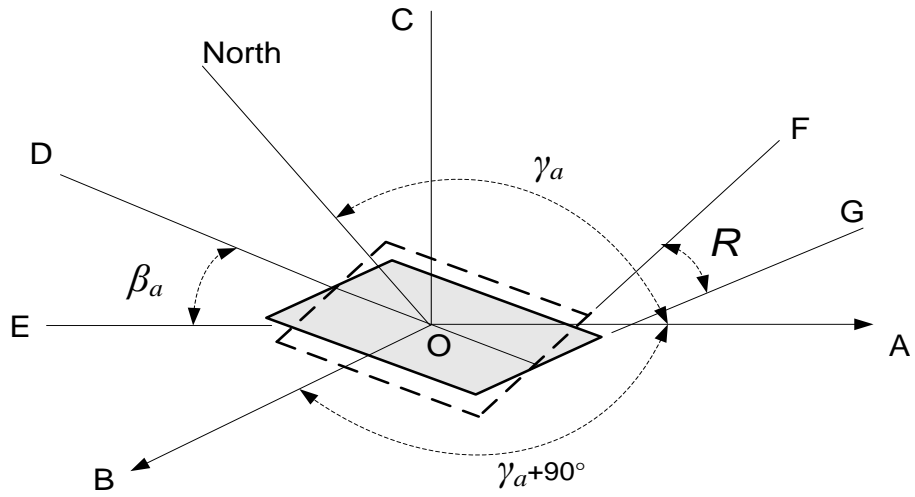
Figure 3.4: Schematic diagram of rotation angle, axis tilt and axis azimuth.

3.4 Tracker tilt angle adjustment:

Several equations and models have been developed to obtain solar radiation on a tilted surface [16]. Using the equations and models solar radiation at a given location and a given time can be plotted against tilt angle, which shows a maxima. Average optimum tilt angle on monthly, seasonally or yearly basis can be determined. Optimum tilt angle can be permanently fixed to one value corresponding to maximum annual solar radiation on the fixed surface, or tilt angle can be adjusted on monthly or seasonal basis for better optimization to maximize annual solar radiation on the collector surface.

Table 3.2 shows optimum tilt angle of solar panel (from horizontal) on monthly basis for Dhaka, Bangladesh which is computed using a solar angle calculator [17].

Table 3.2: Optimum Tilt angle of solar panel (horizontal) for Dhaka, Bangladesh.

Month	Tilt Angle (°)		Month	Tilt Angle (°)
January	40		July	8
February	32		August	16
March	24		September	24
April	16		October	32
May	8		November	40
June	0		December	48

In a study it has been found that the optimum tilt angle for Dhaka, Bangladesh located at 23.7° latitude is 30° [18].

3.5 Determination of Optimum Rotation Angle for Single Axis Tracking:

The cosine of angle of incidence can be expressed as a function of rotation angle [7].

$$cos\theta = cosR[sin\theta_z \cos(\gamma_s - \gamma_a) sin\beta_a + cos\theta_z cos\beta_a] + sinRsin\theta_z sin(\gamma_s - \gamma_a)\ldots\ldots\ldots (3.1)$$
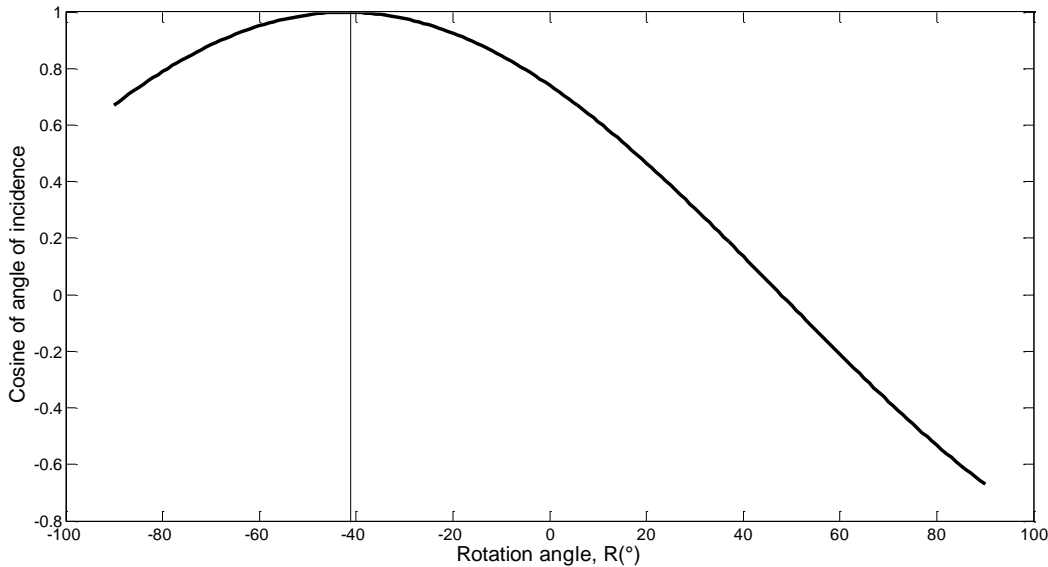
Figure 3.5: Plot of cosine of angle of incidence vs. rotation angle obtained for 9:00 am on September 29, 2016.

At the optimum tracking rotation angle, the incidence angle needs to be minimum, so cosine of incidence angle will be maximum. Figure 3.5 represents cosine of the angle of incidence versus rotation angle curve obtained from equation 1 for $\theta_z = 48.697°$, $\gamma_s = 116.724°$, $\gamma_a = 180°$ and $\beta_a = 24°$ at 9:00 am on September 29, 2016. The values of θ_z and γ_s are obtained from given date, time and location parameters (here, latitude is $+23.69°$, longitude is $-90.36°$ and GMT offset is $+6:00$) using PSA algorithm [14]. The value of β_a is considered for the month of September, according to table 3.2 and the value of γ_a indicates towards which direction the panel is faced. The rotation angle for this graph ranges from -90° to 90°. It is seen that the cosine of the incident angle is maximum, that is the angle of incidence is minimum when $R = -41°$. So the optimum rotation angle R can be found by differentiating equation 1 with respect to R and equating the derivative to zero [7].

$$\frac{d(cos\theta)}{dR} = -sinR[sin\theta_z \cos(\gamma_s - \gamma_a) sin\beta_a + cos\theta_z cos\beta_a] + cosRsin\theta_z sin(\gamma_s - \gamma_a) = 0\ldots\ldots\ldots (3.2)$$

$$\Rightarrow \frac{sinR}{cosR} = \frac{sin\theta_z sin(\gamma_s - \gamma_a)}{sin\theta_z \cos(\gamma_s - \gamma_a) sin\beta_a + cos\theta_z cos\beta_a}$$

$$\Rightarrow R = \tan^{-1} X + \psi\ldots\ldots\ldots\ldots\ldots\ldots\ldots\ldots\ldots\ldots\ldots\ldots\ldots\ldots\ldots\ldots\ldots (3.3)$$

where,

$$X = \frac{sin\theta_z sin(\gamma_s - \gamma_a)}{sin\theta_z \cos(\gamma_s - \gamma_a) sin\beta_a + cos\theta_z cos\beta_a}$$

$\psi = 0° \ if \ X = 0, or \ if \ X > 0 \ and \ (\gamma_s - \gamma_a) > 0, or \ if \ X < 0 \ and \ (\gamma_s - \gamma_a) < 0$

$\psi = +180° \ if \ X < 0 \ and \ (\gamma_s - \gamma_a) > 0$

$\psi = -180° \ if \ X > 0 \ and \ (\gamma_s - \gamma_a) < 0$

To place R in the correct trigonometric quadrant, the variable ψ is used. The difference $(\gamma_s - \gamma_a)$ is evaluated to determine which value of ψ to use so that it falls within the range of -180° to +180° [7].

Chapter 4

Implementation of single axis tracker rotation

4.1 System Architecture and Algorithm
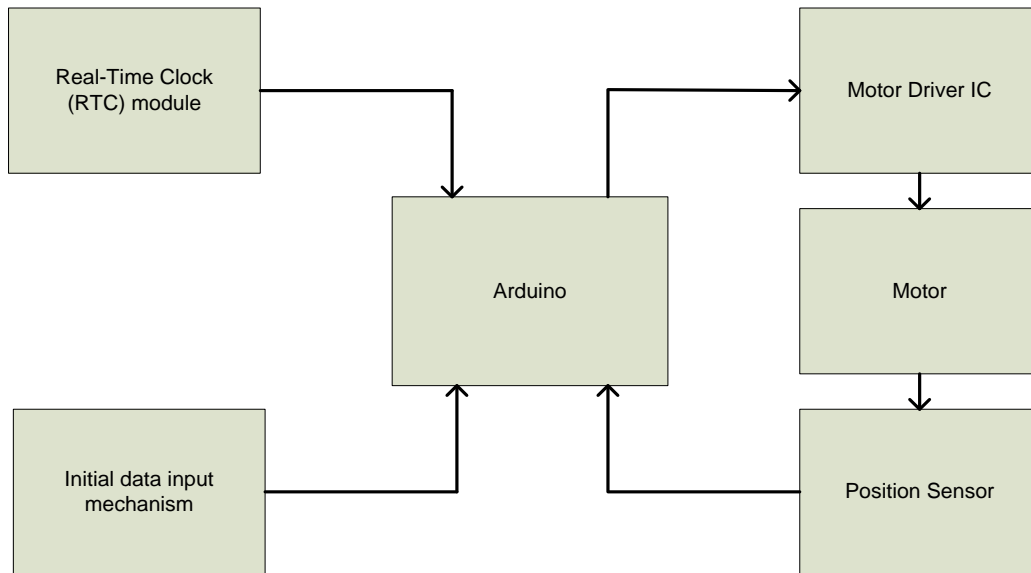
Figure 4.1: Block diagram of open loop tracking system architecture.

Figure 4.1 and 4.2 show the block diagram of system architecture and algorithm flow chart respectively. At the start initial data are entered to the system. The initial data are latitude ('+' entered for location at north of the equator and '-' for location at south of the equator), longitude ('+' for location at west of the prime meridian and '-' for location at east of the prime meridian), GMT offset, tilt, local time and date. In this thesis, the input initialization is achieved through three push button switches and an LCD (Liquid Crystal Display). The push button switches are for increase, decrease and setting purpose respectively. The increase, decrease setting of value for required input, with input name or type is observed in the LCD. The input initialization can also be achieved through keypad and other types of display.

The RTC (Real-Time Clock) is initialized according to the time and date inputs. At the beginning of the tracking loop the arduino reads date and time from RTC and determine solar azimuth and zenith angle by PSA algorithm [14]. From the determined azimuth and zenith the optimum tracker rotation angle is determined using equation 3.3.

Here, rotation angle is limited to tracking range. In our prototype tracking range is from -65° to 65° of rotation angle. That is if the rotation angle is smaller than -65° then it is considered as -65° and if the rotation angle is greater than 65° then it is considered as 65°. Rotation angle is converted to a potentiometer reading value. In our prototype the rotation angle against ADC (Analog to Digital Converter) converted potentiometer values were previously calibrated. Using the calibration data in linear interpolation the arduino-ADC converted potentiometer reading for the required rotation angle is found.
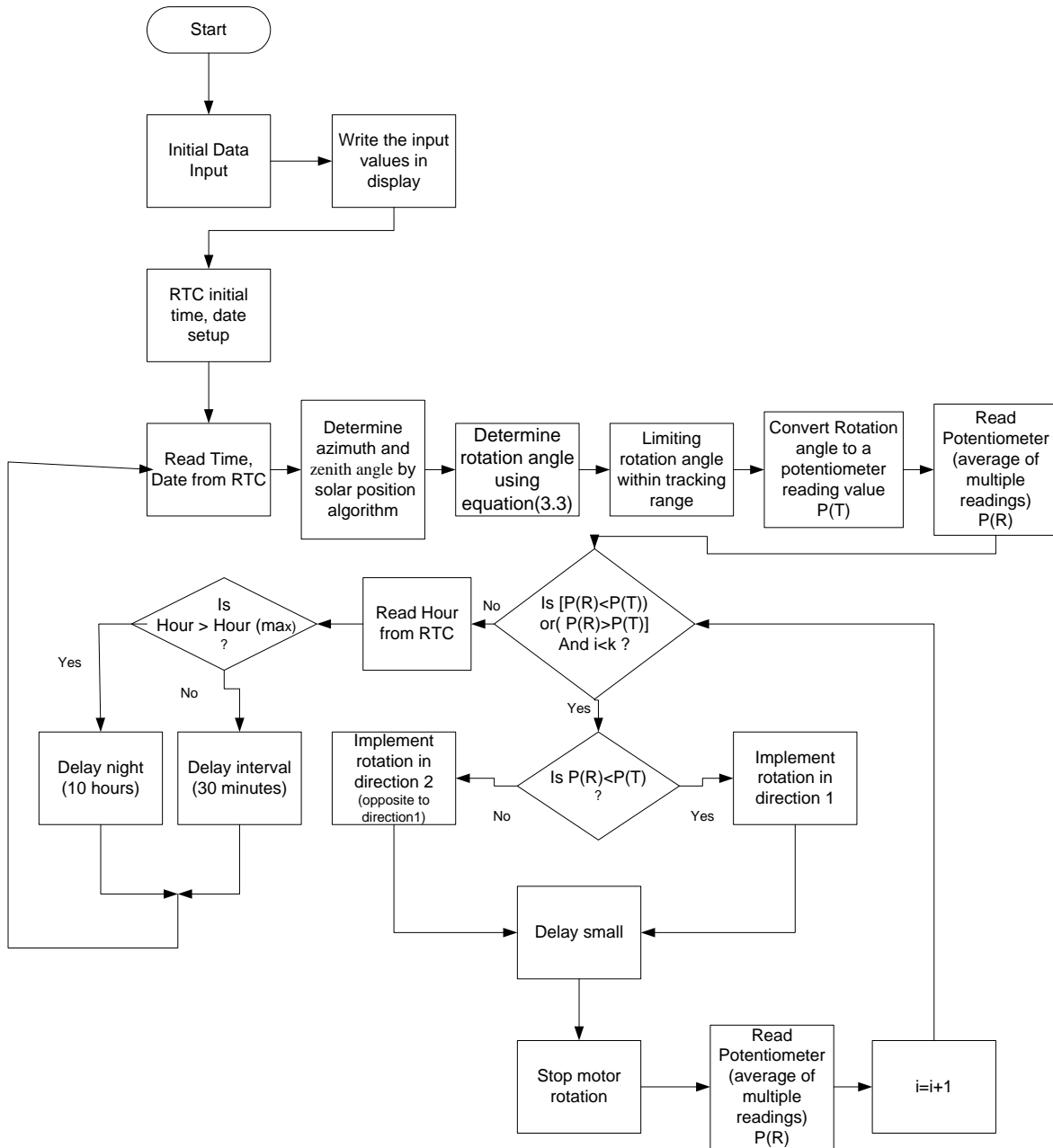
Figure 4.2: Algorithm flow chart for open loop tracking system.

After that arduino-ADC converted current potentiometer reading is taken multiple times. The average of the multiple readings is considered to be the current potentiometer reading P(R). This is done to reduce the impact of noise and fluctuations.

Then P(R) is compared with tracking potentiometer reading P(T) (to be implemented). If P(R) is considerably less than the P(T) then the geared motor controlled by the arduino via motor driver IC moves the collector (panel) in a direction so that the P(R) values moves towards the P(T) values by rotation and if P(R) value is considerably more than P(T) value then the moves the collector in the opposite direction so that the P(R) value moves towards the P(T) value by rotation.

A small delay (in our prototype 100ms) is given to carry out the tracking rotation. The delay should be very small such that within this time the tracking rotation does not pass through two or more calibration points at a time, that is the delay during which the rotation is carried out is to be very small to maintain high resolution of the system to locate a position via a calibration point. After that the motor rotation is stopped and average of multiple potentiometer readings is taken again. The new potentiometer reading at the end again compares with P(T), whether considerably smaller or larger, and similar corresponding action is taken over and over until P(R) value is considerably close or equal to the P(T) value. Thus the tracker obtains the required tracking position.

Here 'i' is a loop control variable. For any disruption the system may not converge to the required calibration point or may oscillate about it. After certain maximum loop iteration represented by 'k' the loop is to be terminated as number of loop iterations i become greater than maximum number of loop iteration k. Thus with loop control variable 'i' in case of any tracking failure the tracker will not be stuck in an infinite loop; the loop gets terminated after certain iteration 'k'.

At the end of each tracking rotation, the hour value from the RTC is read and it is checked whether the hour value from RTC is greater than maximum tracking hour (Hour (max)). In our prototype the 18th hour (6 pm) is considered as maximum time for tracking. If the hour value from RTC is greater than maximum tracking hour then night delay (10 hours in our prototype) is activated. If the hour value is within maximum tracking hour range then interval delay (30 minutes in this case) is activated, that is sun is tracked at certain intervals.

4.2 Components of prototype:

Solar Panel:

The solar panel (Techshop model: SOL-00004) [19] used in the prototype has power rating of 2W. Its working voltage is 9V and operating current is 220mA. Its open circuit voltage and short circuit current are 9.6V and 500mA respectively. It can operate within -40°C~80°C temperature range. A photographic view of the panel is provided in figure 4.3.

Figure 4.3: Photographic view of a solar panel.

Arduino Uno:

Arduino Uno [20] is ATmega328/328P [21] based microcontroller board. Its operating voltage is 5V and DC current received or provided by per I/O pins is 20mA, the maximum current value can be 40mA. For 3.3V pin the current is 50mA. It contains 14 digital input/output pins and 6 analog pins. Out of 14 digital input/output pins 6 pins provide PWM output. For analog inputs AREF pin can be used as analog reference. It has a clock speed of 16MHz, flash memory of

32kB of which 0.5kB is used by bootloader, SRAM of 2kB and EEPROM of 1kB. Figure 4.4(a) and 4.4(b) show the schematic view of Arduino and ATmega 382 with arduino mapping respectively.

(a)   (b)
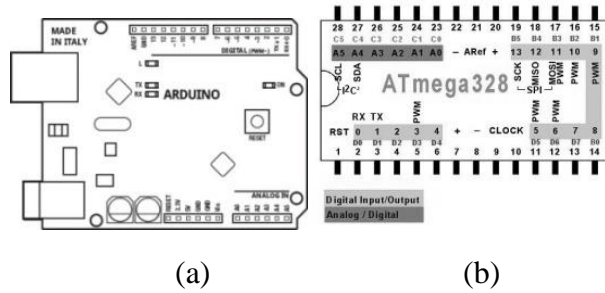
Figure 4.4: Schematic view of (a) Arduino Uno board, (b) ATmega 328 with arduino mapping.

RTC Module:

The RTC module (Techshop model: MOD-00078) [19] used for making the prototype is based on DS1307 [22] Real Time Clock. The RTC has 56 bytes of battery-backed SRAM and uses external 32.768kHz crystal. It manages all timekeeping functions and has calendar validity up to 2100. Figure 4.5(a) represents the photographic view of RTC module and 4.5(b) shows schematic view of DS1307. Table 4.1 shows the pin functions of DS1307 [22].

(a)   (b)
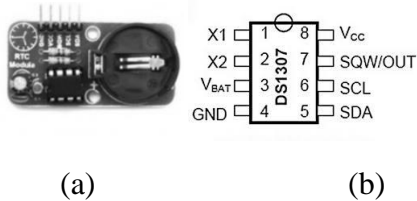
Figure 4.5: (a) Photographic view of an RTC module, (b) Pin diagram of DS1307.

Table 4.1: Functions of DS1307 pins.

Pins	Description
V_{CC}	Primary Power Supply
X_1, X_2	32.768kHz Crystal Connection
V_{BAT}	+3V battery input
GND	Ground
SDA	Serial data, input/output pin for the 2-wire serial interface
SCL	Serial clock, used to synchronize data movement on the serial interface
SQW/OUT	Square wave/Output driver

Motor Driver IC:

The L293D device is used in this thesis to control the motor movement. It can provide bidirectional drive currents of up to 600mA at voltages from 4.5V to 36V. It can operate within 0°-70°C range. Its pin diagram and pin functions [23] are provided in figure 4.6 and table 4.2 respectively.
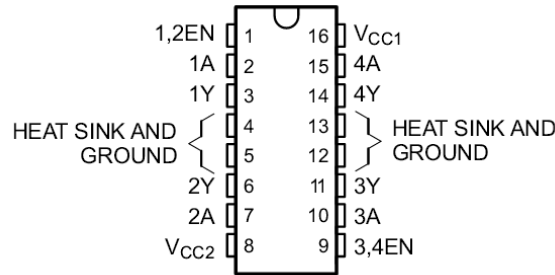
Figure 4.6: Pin diagram of L293D motor driver IC.

Table 4.2: Pin functions of the motor driver IC.

Pin		Functions
Name	Number	
1,2EN	1	Enable driver channels 1 and 2 (active high input)
1A, 2A, 3A, 4A	2, 7, 10, 15	Driver inputs, non inverting
1Y, 2Y, 3Y, 4Y	3, 6,11, 14	Driver outputs
Heat sink and ground	4, 5, 12, 13	Device ground and heat sink pin, connect to printed-circuit-board ground plane with multiple solid vias
3,4EN	9	Enable driver channels 3 and 4 (active high input)
V_{CC1}	16	5-V supply for internal logic translation
V_{CC2}	8	Power VCC for drivers 4.5 V to 36 V

If the motor terminals are connected to 1A and 2A provided that enable pin 1,2EN is set to HIGH logic, the motor driver will follow the truth table [24] provided in table 4.3.

Table 4.3: Truth table for motor driver IC.

1A	2A	Description
0	0	Motor stops
0	1	Motor runs anti-clockwise
1	0	Motor runs clockwise
1	1	Motor stops

DC gear motor:

This motor (Techshop model: ROB-00076) [19] has rated voltage of 12V and rotation speed of 11rpm at no load condition. It provides a torque of 2.65Nm at rated voltage and current of 200mA. Its photographic view is provided in figure 4.7.

Figure 4.7: Photographic view of a DC gear motor.

Multi turn wire-wound potentiometer:

A 10 turn wire-wound potentiometer (model: 35905-2-103, brand: Baoter) [25] is used to determine position of the panel. It has ±5% standard tolerance and ±0.25% linearity. Its excess noise ratio is 200ΩENR. It works within -55°C to 100°C temperature range. Figure 4.8 shows its photographic view.

Figure 4.8: Photographic view of multi turn wire-wound potentiometer.

LCD:

A 16*2 LCD (Techshop model: DIS-00003) [19] is used to display the input data provided to the arduino. It is powered by 5V. In this prototype data is transferred using only 4 buses of DB_4-DB_7. Its schematic diagram and pin connections are provided in figure 4.9 and table 4.4 respectively.
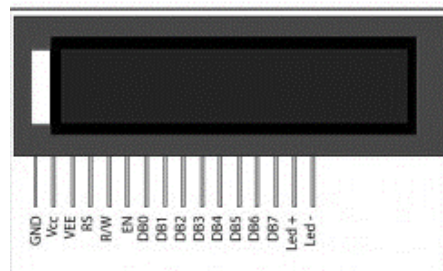
Figure 4.9: Schematic view of an LCD.

Table 4.4: Pin functions of LCD.

Pin number	Symbol	Level	Function
1	V_{SS}	-	0V
2	V_{DD}	-	5V
3	V_O	-	Variable voltage
4	RS	H/L	L:Instruction Code Input
			H: Data Input
5	R/W	H/L	H: Data read
			L:Data Write
6	E	H,H→L	Enable signal
7	DB0	H/L	Data Bus Lines
8	DB1	H/L	
9	DB2	H/L	
10	DB3	H/L	
11	DB4	H/L	
12	DB5	H/L	
13	DB6	H/L	
14	DB7	H/L	

Chapter 5

Performance analysis of single axis tracker rotation:

5.1 Experimental Setup for measurement:

When the normal to collector surface is parallel to vertical plane, the position is considered as the reference position, where $R = 0°$. R is positive for clockwise rotation and negative for counterclockwise rotation. The tracker is allowed to rotate within -65°<R<65°.

A printed protractor is attached about the axis of the prototype and a pointer is attached in alignment with the collector surface for measuring rotation angle as shown in figure 5.1(a) and 5.1(b). The rotation angle is measured on September 29, 2016 by observation. The measured values are compared with NREL-SPA extracted values for that day to determine the accuracy.

(a)   (b)
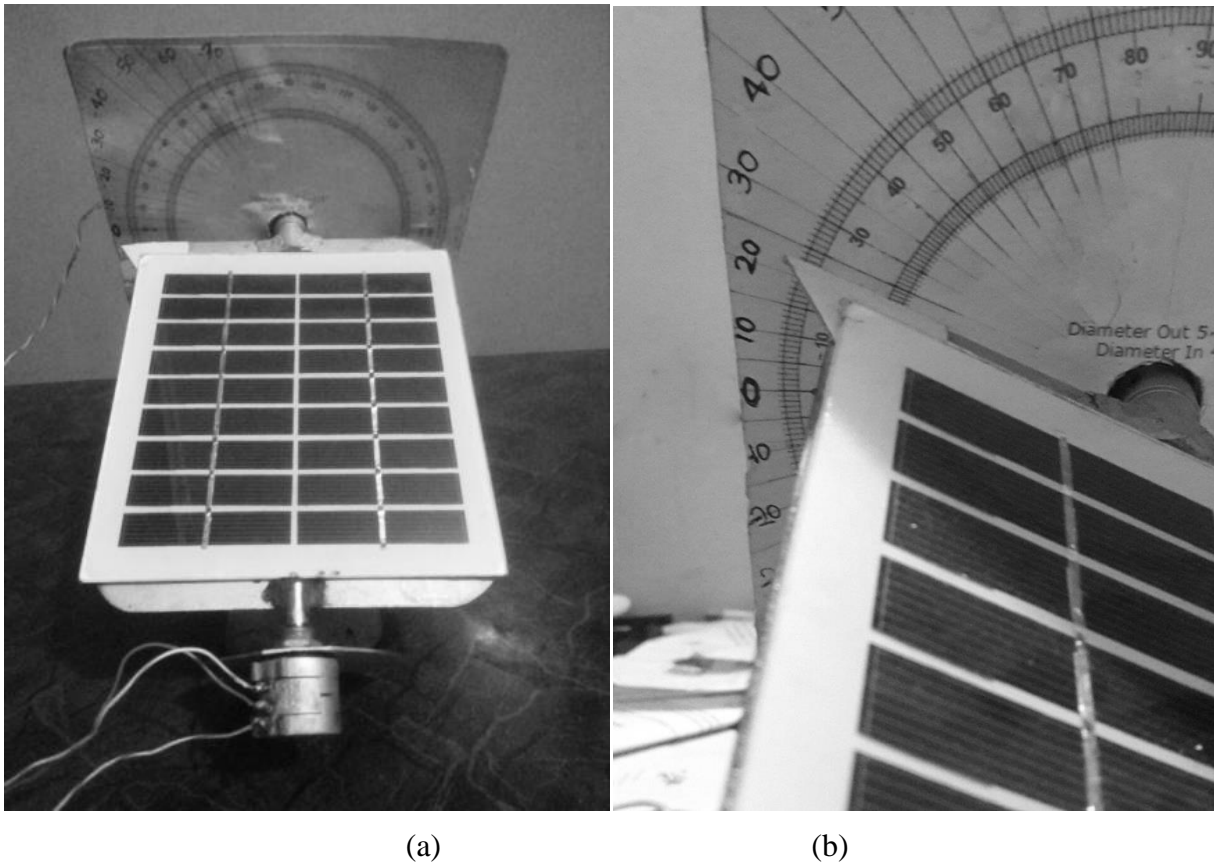
Figure 5.1: (a) Setup for tracker position measurement, (b) Rotation angle measured at $R = 21°$ at 13:24 on September 29, 2016.

5.2 Results and discussions:

Table 5.1: Comparison of rotation angle from measurement and NREL-SPA data for September 29, 2016.

| Time	Rotation angle (Measured) (°)	Rotation angle (NREL) (°)	Error (°)
8:14	-57	-53.43	-3.57
8:45	-48	-45.73	-2.27
9:16	-41	-38.01	-2.99
9:46	-33	-30.5	-2.5
10:17	-25	-22.76	-2.24
10:48	-20	-15.0	-5
11:19	-12	-7.22	-4.78
11:50	-5	-5	0
12:21	5	8.33	-3.33
12:53	14	16.36	-2.36
13:24	21	24.12	-3.12
13:55	28	31.87	-3.87
14:26	38	39.60	-1.6
14:57	46	47.36	-1.36
15:28	54	55.05	-1.05
15:59	62	62.72	-0.72
16:30	69	70.37	-1.37

According to table 5.1 and figure 5.2 error between measured and computed rotation angle from NREL data range within 5°. It is also observed that measured values are always less than NREL values and the errors are always negative. This pattern of error has occurred because the rotation values to which potentiometer readings are calibrated have shifted slightly from the actual values of rotation angle in measurement in one direction such that during measurement the calibrated rotation values are slightly less than actual rotation values. Such calibration error occurs due to small displacement of the components by shock or vibration.
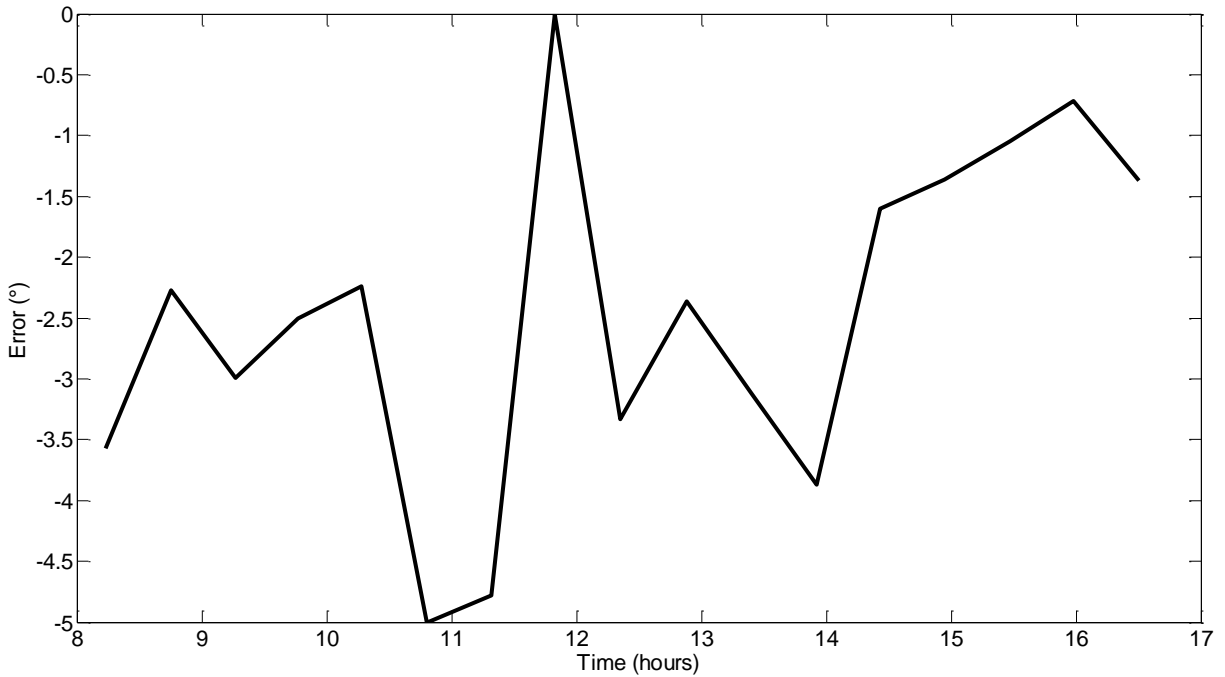
Figure 5.2: Plot of time vs. error from the data collected on September 29, 2016.

To minimize the error, the mounting and DC motor-potentiometer coupling should be strong and suitable such that it can resist the effect of shock and vibration during the operation. In DC motor-potentiometer coupling we can use a gear which can increase the potentiometer angular displacement with respect to certain DC motor angular displacement at a particular direction. This will improve the resolution and thus the error can be minimized. Besides, optimization of the motor speed and torque through simulation of the mechanical system can give further provision for minimizing the error.

Chapter 6

Improved energy harvesting by the solar tracker

6.1 Experimental process and measurement

To determine improvement in energy extraction by solar tracker, two identical panels of 2W (tracker panel and fixed panel) are taken for solar tracking panel system and fixed panel system respectively. Both the panels are tilted at 32° and faced towards the south. The experiment is conducted on November 4, 2016 on a building roof located at 23.70016° N, 90.3723° E, Dhaka Bangladesh from a height of 16m. The open circuit voltage and short circuit current of both the panels are recorded at 30 minutes interval from 6:45 am to 4:15 pm.

Despite of panels being identical, there is panel to panel V_{OC} (open circuit voltage) fluctuation. To remove this fluctuation for comparison V_{OC} of one panel needs to be scaled according to V_{OC} of other panel. Here, with respect to open circuit voltage of tracker panel $V_{OC(T)}$ fixed panel open circuit voltage $V_{OC(F)}$ is scaled. Keeping position of the panels, time and other parameters same $V_{OC(T)}$ is divided by $V_{OC(F)}$ to obtain fixed panel to tracker panel conversion ratio and then fixed panel open circuit voltage measurements are multiplied with this conversion ratio value to obtain the scaled fixed panel open circuit voltage $V_{OC(F1)}$ values. Similarly to remove I_{SC} (short circuit current) fluctuation for comparison, the fixed panel to tracker panel conversion ratio is calculated to scale the fixed panel $I_{SC(F)}$ with respect to tracker panel $I_{SC(T)}$. Multiplying the fixed panel $I_{SC(F)}$ measurements with this conversion ratio, scaled fixed panel $I_{SC(F1)}$ values are obtained.

The identical panels have same fill factor ($F=V_{M}I_{M}/V_{OC}I_{SC}$), where V_M and I_M are voltage and current respectively at maximum power, V_{OC} and I_{SC} are obtained from specifications data. At a particular time maximum power obtained from tracker panel ($P_{M\ (T)}$) is calculated from the following equation.

$$P_{M(T)}(mW) = V_{OC\ (T)}(V) \times I_{SC\ (T)}(mA) \times F \dots\dots\dots\dots\dots\dots\dots\dots\dots\dots\dots\dots\dots\dots\dots\dots\dots\dots (6.1)$$

Similarly, maximum power obtained from tracker panel ($P_{M\ (F1)}$) is calculated from

$$P_{M(F1)}(mW) = V_{OC\ (F1)}(V) \times I_{SC\ (F1)}(mA) \times F \dots\dots\dots\dots\dots\dots\dots\dots\dots\dots\dots\dots\dots\dots\dots\dots\dots (6.2)$$

Thus maximum power from each panel at 30 minutes interval is calculated and plotted against time. From the curve the energy extracted from each panel can be computed and compared.

6.2 Results and Discussions:

Table 6.1: Power obtained from tracker panel and fixed panel at different times.

| Time	Cloud condition	$V_{OC(T)}$ (V)	$I_{SC(T)}$ (mA)	$V_{OC(F1)}$ (V)	$I_{SC(F1)}$ (mA)	Fill factor, F	$P_{M(T)}$ (mA)	$P_{M(F1)}$ (mA)
6:45am	Free of cloud over sun position	9.22	14.4	8.52	9		54.77	31.63
7:15 am		9.8	85.4	9.41	27		345.23	104.80
7:45 am		9.81	129	9.7263	58		522.01	232.70
8:15 am		9.83	150.8	9.8677	87.09		611.48	354.49
8:45 am		9.74	170.3	9.8374	118.1		684.22	479.24
9:15 am		9.72	178	9.8273	138		713.69	559.42
9:45 am		9.73	187	9.8778	158		750.55	643.79
10:15 am		9.7	188	9.8273	169		752.24	685.09
10:45 am		9.76	181	9.8172	173.16		728.71	701.23
11:15 am		9.67	181	9.6556	180.1		721.99	717.33
11:45 am		9.7	196	9.696	195		784.25	779.92
12:15 am	Heavy cloud over sun position	9.41	49	9.2516	49		190.20	187
12:30 pm	Partially free of cloud over sun position	9.95	142	9.898	139	0.4215	582.82	567.53
12:45 pm	Free of cloud over sun position	9.79	196.3	9.7263	192.4		792.73	771.93
1:15 pm		9.57	171.4	9.5243	161.9		676.62	636.07
1:45 pm	Heavy cloud over sun position	9.33	32	9.1506	29.3		123.16	110.60
2:15 pm	Partially free of cloud over sun position	9.69	136.7	9.59	116		546.41	458.88
2:45 pm		9.5	90.5	9.393	72.4		354.65	280.52
3:15 pm		9.66	103.5	9.5647	79.1		412.42	312.08
3:30 pm		9.57	72.5	9.3526	53.7		286.20	207.17
3:45 pm		9.11	23.8	8.7971	18.3		89.44	66.41
4:15 pm	Heavy cloud over sun position	8.05	5.2	8.13	5.2		17.27	17.44
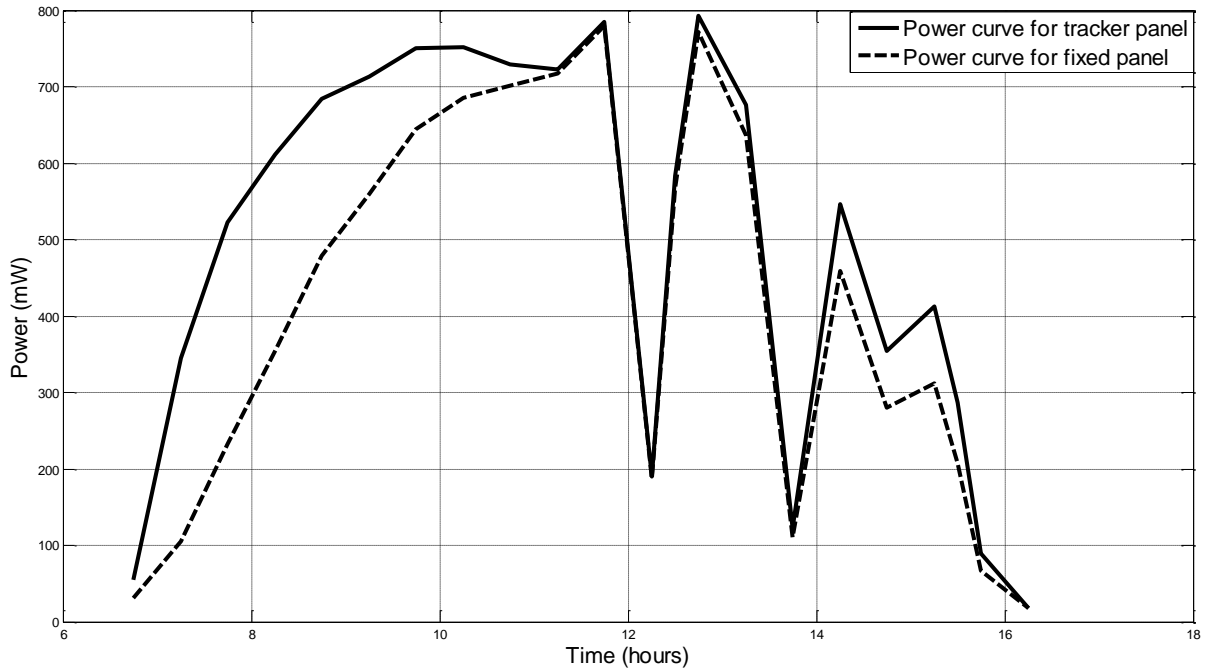
Figure 6.1: Plot of power vs. time for tracker panel and fixed panel.

Table 6.1 and figure 6.1 show data of power obtained from tracker and fixed panels at different times and power versus time curve for both panels. Using trapezoidal numerical integration in MATLAB, energy extracted by tracker panel and fixed panel from 6:45 am to 4:15 pm are computed as 4949mWh and 4079.5mWh respectively. With respect to fixed panel system, about 21% higher energy is obtained from solar tracker PV system. During this experiment cloud has covered the sun position for more than 30% of the experiment day. In clear sky condition, the percentage of improved energy harvesting will be evidently more.

Chapter 7

Conclusion

7.1 Summary

In this thesis work we have developed an open loop single axis solar tracker system for improved energy extraction with the implementation of optimum panel rotation. The performance of the tracker system and energy obtained from this system with respect to fixed PV system are observed.

The rotation angle of the panel is determined using time, date, location parameters and selected algorithm and compared with the rotation angle computed from NREL data (considered as benchmark for this thesis). The variations have been within ±5° which has ensured that expected performance of the tracker is achieved. Also, energy obtained from tracker system and fixed panel system are determined and evaluated over a day. 21% more energy extraction from the tracker panel with respect to fixed panel system has been witnessed on a 30% overcast day.

7.2 Future development

The prototype developed for the demonstration of the idea employs Arduino Uno as control unit. With arduino the device is not suitable for commercialization because it is not economically scalable with arduino. So for making the device economically scalable and suitable for commercialization the control program needs to be transferred to a microcontroller chip. As Arduino Uno uses ATmega328/328P [21] microcontroller chip, it is most convenient to transfer the operating program to this chip. For commercialization, the device also needs a rigid and robust mounting structure. If manually adjustable tilt at different pre-defined position on seasonal basis is provided in the mounting structure, this will give scope for better optimization of tilt angle and also maximize the radiation on the collector surface over a period. In the prototype the coupling between DC motor and wire-wound potentiometer is slightly affected by shock and vibration during operation. A robust gear coupling which is immune to shock and vibration can be used here to improve the performance of the device. For outdoor installation certain protective measures in the mounting and installment need to be taken from rain, storm and other possible hazards.

The performance of the prototype with proper speed and torque control needs to be mechanically simulated for better optimization of speed and torque of the DC motor. Besides, the computation of the rotation angle can be more optimized by using a simpler solar position algorithm (compared to PSA algorithm, used for the prototype) which can determine solar zenith and azimuth angles with optimum accuracy over a desired period of time.

References

[1] G. M. Masters, "The solar resource," in *Renewable and Efficient Electric Power Systems*. Hoboken, New Jersey: Wiley & Sons, Inc., 2004, ch. 7, pp. 410-416.

[2] O. Bingol, Y. Önerl A. Altinta, "Microcontroller based solar-tracking system and its implementation," *J. of Eng. Sci.*, vol. 12, no. 2, pp. 243-248, 2006.

[3] S. Kivrak, M. Gunduzalp, F. Dincer, "Theoretical and experimental performance investigation of a two-axis solar tracker under the climatic condition of Denizli, Turkey," *Przegląd Elektrotechniczny*, vol. 2012, no. 2, pp. 332-336, 2012.

[4] B. J. Huang, W. L. Ding, Y. C. Huang, "Long-term field test of solar PV power generation using one-axis 3-position sun tracker," *Solar Energy*, vol. 85, no. 9, pp. 1935–1944, Sept. 2011.

[5] F. R. B. Karim, Md. M. Rashed, M. Quamruzzaman, "Design and implementation of a sensorless dual axis solar tracking system based on solar sun chart algorithm using arduino," in *Electrical Communication Engineering and Renewable Energy*, Chittagong, Bangladesh, 2014, pp. 126-130.

[6] M. I. Rashid, M. F. Akorede, L. Z. Chao and N. F. N. Mohammed, "Dual-axis solar tracking system for maximum power production in PV systems," *Nigerian J. of Technological Develop.*, vol. 12, no. 2, pp. 42-47, Dec. 2015.

[7] W. F. Marion and A. P. Dobos, "Rotation angle for the optimum tracking of one-axis tracker," Nat. Renewable Energy Laboratory, Denver, CO, Tech. Rep. NREL/TP-6A20-58891, 2013.

[8] J. M. Wang and C. L. Lu, "Design and implementation of a sun tracker with a dual-axis single motor for an optical sensor-based photovoltaic system," *Sensors*, vol. 13, no. 3, pp. 3157-3168, Mar. 2013.

[9] J. Meeus, *Astronomical Algorithms*, 2nd ed. Richmond, Virginia: Willmann-Bell, Inc., 1998.

[10] I. Reda and A. Andreas, "Solar position algorithm for solar radiation applications," National Renewable Energy Laboratory, Denver, CO, Tech. Rep. NREL/TP-560-34302, 2008.

[11] Nautical Almanac Office, *The Astronomical Almanac 2004*. Norwich, United Kingdom: TSO, 2003.

[12] R. Grena, "An algorithm for the computation of the solar position," *Solar Energy*, vol. 82, no. 5, pp. 462-470, May 2008.

[13] J. J. Michalsky, "The Astronomical Almanac's algorithm for approximate solar position (1950–2050)," *Solar Energy*, vol. 40, no. 3, pp. 22-235, December 1988.

[14] M. Blanco-Muriel, D. C. Alarcón-Padilla, T. López-Moratalla, M. Lara-Coira, "Computing the solar vector," *Solar energy*, vol. 70, no. 5, pp. 431-441, 2001.

[15] R. Grena, "Five new algorithms for the computation of sun position from 2010 to 2110," *Solar Energy*, vol. 86, no. 5, pp. 1323-1337, May 2012.

[16] M. J. Ahmad and G. N. Tiwari, "Optimization of tilt angle for solar collector to receive maximum radiation," *The Open Renewable Energy J.*, vol. 2, no. 1, pp. 19-24, Feb. 2009.

[17] The solar electricity handbook. [Online]. http://solarelectricityhandbook.com/solar-angle-calculator.html

[18] H. R. Ghosh, S. B. Alam, U. K. Das, A. Sen, D. Datta, "Surface orientations and energy policy for solar module applications in Dhaka, Bangladesh," *Int. J. Scientific & Eng. Research*, vol. 5, no. 2, pp. 283-288, Feb. 2014.

[19] Techshop Bangladesh. [Online]. https://www.techshopbd.com/

[20] Arduino. [Online]. https://www.arduino.cc/en/Main/ArduinoBoardUno

[21] Atmel Corporation. [Online]. http://www.atmel.com/Images/Atmel-42735-8-bit-AVR-Microcontroller-ATmega328-328P_Datasheet.pdf

[22] Spark fun Electronics. [Online]. https://www.sparkfun.com/datasheets/Components/DS1307.pdf

[23] Texas Instruments. [Online]. http://www.ti.com/lit/ds/symlink/l293.pdf

[24] Mobilina Robotika. [Online]. http://robotika.yweb.sk/skola/H-brigde/IC%20L293%20and%20Its%20avr%20%20interface%20v1.0.pdf

[25] Lion Electronics. [Online]. http://www.lion.co.il/site/HvDest/3590%20series.pdf

Appendix

A.1 Nomenclature of the angles

γ_s	Solar azimuth angle
θ_z	Zenith angle
ε	Elevation angle
θ	Angle of incidence
β_a	Axis tilt
γ_a	Axis azimuth
R	Rotation angle